RESEARCH PAPER

Investigation of the Effect of Hydroxypropyl Methylcellulose on the Phase Transformation and Release Profiles of Carbamazepine-Nicotinamide Cocrystal

Mingzhong Li • Shi Qiu • Yan Lu • Ke Wang • Xiaojun Lai • Mohammad Rehan

ABSTRACT

Purpose The aim of this work was to investigate the influence of hydroxypropyl methylcellulose (HPMC) on the phase transformation and release profile of carbamazepine-nicotinamide (CBZ-NIC) cocrystal in solution and in sustained release matrix tablets.
Methods The polymorphic transitions of the CBZ-NIC cocrystal and its crystalline properties were examined by differential scanning calorimetry (DSC), X-ray powder diffraction (XRPD), Raman spectroscopy, and scanning electron microscopy (SEM).
Results The apparent CBZ solubility and dissolution rate of CBZ-NIC cocrystal were constant in different concentrations of HPMC solutions. In a lower percentage of HPMC in the matrix tablets, the CBZ release profile of the CBZ-NIC cocrystal was nonlinear and declined over time. With an increased HPMC content in the tablets, the CBZ-NIC cocrystal formulation showed a significantly higher CBZ release rate in comparison with the other two formulations of CBZ III and the physical mixture.
Conclusions Because of a significantly improved dissolution rate of the CBZ-NIC cocrystal, the rate of CBZ entering into solution is significantly faster than the rate of formation of the CBZ-HPMC soluble complex in solution, leading to a higher supersaturation level of CBZ and subsequently precipitation of CBZ dihydrate.

KEY WORDS carbamazepine-nicotinamide (CBZ-NIC) cocrystal · hydroxypropyl methylcellulose (HPMC) · inhibition · phase transformation · UV imaging

M. Li (✉) · S. Qiu · Y. Lu · K. Wang
School of Pharmacy, De Montfort University, Leicester
Leicester LE1 9BH, UK
e-mail: mli@dmu.ac.uk

X. Lai · M. Rehan
School of Process, Environmental and Materials Engineering
University of Leeds, Leeds LS2 9JT, UK

INTRODUCTION

Enhancing the solubility and dissolution rates of poorly water soluble compounds has been one of the key challenges for the successful development of new medicines in the pharmaceutical industry over decades. There are many developed methods (such as solid dispersion, micronisation, and salt formation) but pharmaceutical cocrystals (made by forming a crystal of a drug in combination with a coformer with a specific stoichiometric composition) have been recognised as an alternative approach with enormous potential to provide new and stable structures of the active pharmaceutical ingredients (APIs) (1,2). Although pharmaceutical cocyrstals can offer the advantages of providing a higher dissolution rate and greater apparent solubility to improve the bioavailability of a poorly water soluble drug, a key limitation to the approach is that a stable form of the drug can be recrystallized during the dissolution of the cocrystals, resulting in the loss of the improved drug properties. For example, in our previous study we have shown that the solution mediated phase transformation of the carbamazepine-nicotinamide (CBZ-NIC) cocrystal had greatly reduced the enhancement of its apparent solubility and dissolution rate (3). In order to inhibit the form conversion of the cocrystals in aqueous media, recent studies have shown that the inclusion of a surfactant in the formulation as the potential to overcome the limitations caused by the rapid dissociation of cocrystals and concomitant recrystallization of the poorly soluble forms in aqueous media (4–6). Obviously careful selection of both the cocrystal form and the excipients is an essential part of successful product development. More research is needed to explore the functions of excipients in formulations to maximise the benefit of cocrystals.

Carbamazepine (CBZ) is an Anti-epilepsy drug that has been used for many decades. Anhydrous CBZ III is classified as a class II drug according to the BCS classification due to its low solubility and high permeability (7). Many studies have

been carried out to form CBZ cocrystals to improve its solubility and dissolution behaviour (8). In this work, carbamazepine and nicotinamide (NIC) were selected as the model drug and coformer to investigate the crystalline properties and dissolution rate of the CBZ-NIC cocrystal in sustained release formulations based on hydroxypropyl methylcellulose (HPMC) and in aqueous solutions. It is well known that when CBZ III is suspended in water it rapidly transforms to the dihydrate. Previous work has shown that HPMC inhibits the transformation of CBZ III to CBZ dihydrate (CBZ DH) in the gel layer of hydrated tablets and in aqueous solutions (9). The mechanism of the effects of HPMC was due to the interaction between the drug and polymer through hydrogen bonding. The hydroxyl groups of HPMC attaches to CBZ at the site of water binding, resulting to inhibiting its transformation to the dihydrate form. The present work is part of a study to understand the factors that affect the cocyrstal dissolution behaviour, in particular the solution mediated phase transformation. Key questions to be addressed are whether HPMC can have a similar function to inhibit CBZ recrystallization from solution during CBZ-NIC cocrystal dissolution. Through comparison of the crystalline properties and dissolution profiles of the CBZ-NIC cocrystal, CBZ III alone and a physical mixture of CBZ III and NIC in both HPMC matrices and in aqueous solutions, we aimed to elucidate the effect of HPMC on the drug release profile in a cocrystal sustained release formulation and the possible interaction mechanism between CBZ and HPMC in solution. The influence of HPMC on the polymorphic transitions of the CBZ-NIC cocrystal and its crystalline properties were examined by differential scanning calorimetry (DSC), X-ray powder diffraction (XRPD), Raman spectroscopy, and scanning electron microscopy (SEM).

MATERIALS AND METHODS

Materials

Anhydrous CBZ (CBZ III) was purchased from Zhenjiang Jiuzhou Pharmaceutical Co., Ltd (Taizhou, China). Nicotinamide (NIC) (≥99.5% purity) was purchased from Sigma-Aldrich (Dorset, UK). Hydroxypropyl methylcellulose (HPMC) (Hypromellose 900SH-4000) was provided by Shin-Etsu Pharma& Food Materials Distribution GmbH (Stevenage, UK) as an in-kind contribution. Sodium lauryl sulphate (SLS) (≥99%) and methanol (HPLC grade) were purchased from Fisher Scientific (Loughborough, UK) and used as received. Double distilled water was generated from a Bi-Distiller (WSC044.MH3.7, Fistreem International Limited, Loughborough, UK) and used throughout the study.

Methods

Formation of Carbamazepine and Nicotinamide (CBZ-NIC) Cocrystal

The CBZ-NIC cocrystal was prepared by the reaction crystallisation method. A 1:1 molar ratio mixture of CBZ III and NIC was completely dissolved in Ethyl acetate (EtOAc) with aid of stirring at 70°C. The solution was put in the ice bath for 2 h and then the suspension was filtered through 0.45 μm filters (thermo Scientific Nalgene) to collect the solid residuals of CBZ-NIC cocrystal. X-ray powder diffraction (XRPD), Raman spectroscopy, and differential scanning calorimetry (DSC) were used to confirm the formation of the cocrystals.

Preparation of Tablets

The formulations of the matrix tablets are provided in Table I. Cylindrical tablets were prepared by direct compression of the blends, using a laboratory press fitted with a 13 mm flat-faced punch and die set and applying 1tonforce. All tablets contained the equivalent 200 mg CBZ III.

Intrinsic Dissolution Study by UV Imaging System

The dissolution behaviour of CBZ III and the CBZ-NIC cocrystal in pure water and different concentrations of HPMC solutions was studied using an ActiPix SDI 300 UV surface imaging system (Paraytec Ltd., York, UK). It comprises of a sample flow cell, syringe pump, temperature control unit, UV lamp and detector, and control and data analysis system, which was the same as that used in our previous studies (3,5). UV imaging calibration was performed by imaging a series of CBZ standard solutions in pure water with concentrations of 4.23×10^{-3} mM, 2.12×10^{-2} mM, 4.23×10^{-2} mM, 8.46×10^{-2} mM, 1.69×10^{-1} mM, and 2.54×10^{-1} mM. A standard curve was constructed by plotting the absorbance against concentration of each standard solution based on three repeated experiments. The calibration curve was validated by a series of CBZ standard solutions with different HPMC concentrations, showing that HPMC did not affect the accuracy of the model and that the calibration curve was applicable for the dissolution test with HPMC solutions. The sample compact in a dissolution test was made by filling around 5 mg of the sample into a stainless steel cylinder (inner diameter: 2 mm) and compressed by a Quickset MINOR torque screwdriver (Torqueleader, M.H.H. engineering Co. Ltd., England) for 1 min at a constant torque of 40cNm. All dissolution tests were performed at 37 ± 0.5°C and the flow rate of a dissolution medium was set at 0.4 ml/min in this study. The concentrations of HPMC

Table I Matrix Tablet Composition (mg)

Component	Formulation					
	F1	F2	F3	F4	F5	F6
CBZ III	200			200		
CBZ-NIC cocrystal		304			304	
Equal molar physical mixture of CBZ III and NIC			304			304
HPMC K4M	100	100	100	200	200	200

solutions were 0, 0.5, 1, 2, 5 mg/ml. Each sample has been tested for 1-h in triplicate.

Solubility Analysis of CBZ-NIC Cocrystal, CBZ III and Physical Mixture of CBZ III and NIC in HPMC Solutions

An excess of CBZ-NIC cocrystal, CBZ III and the physical mixture of CBZ III and NIC, all of which were slightly grinded and sieved by 60 mesh sieve (250 μm), were added into a small vial containing 10 mL of dissolution media with different concentrations of HPMC and shaken with stirring for 24 h. Aliquots were filtered through 0.45 μm filters (thermo Scientific Nalgene) and diluted properly for determination of the concentrations of CBZ and NIC by HPLC. Solid residues were retrieved from the tests, dried at room temperature for 1 day, and analyzed by DSC, Raman and SEM. The media used for the tests included water, 0.5, 1, 2 and 5 mg/ml HPMC solutions.

Dissolution Studies of Formulated HPMC Matrix Tablets

The dissolution tests of the tablets were carried out by the USP I basket method for 6 h. Rotation speed was 100 rpm and the dissolution medium was 700 ml of 1% SLS aqueous solution to achieve sink conditions, maintained at 37 ± 0.5°C. Samples of 5 ± 0.1 ml were taken manually at 0.5, 1, 2, 3, 4, 5 and 6 h replaced with an equal volume of the fresh medium to maintain a constant dissolution volume. The samples were filtered and measured by HPLC to determine the concentrations of CBZ and NIC. The dissolution profiles were represented as the cumulative percentages of the amount of drug released at each sampling interval. Each profile is the average of three individual tablets.

After a dissolution test, the solid residues were collected and dried at room temperature for at least 24 h for the further analysis of XRPD, DSC, and SEM.

Physical Properties Characterisation Techniques

High Performance Liquid Chromatography (HPLC)

The concentrations of CBZ and NIC in a solution were analysed by Perkin Elmer series 200 HPLC system. A

HAISLL 100 C18 column (5 μm, 250×4.6 mm) (Higgins Analytical, Inc. USA) at ambient temperature was used. The mobile phase was composed of 70% methanol and 30% water, and the flow rate was 1 mL/min using an isocratic method.

Raman Spectroscopy

An EnSpectr R532® Raman spectrometer (Enhanced Spectrometry, Inc., Torrance, USA) was used to measure the solid residues after the solubility tests. The measurements were carried out at room temperature using a 20–30 mW output power laser source with a wavelength of 532 nm. The integration time was 200 milliseconds and each spectrum was obtained based on an average of 50 scans. In order to quantify the percentage of CBZ dihydrate (CBZ DH) crystallised during the solubility tests, CBZ III and the CBZ-NIC cocrystal were blended separately with CBZ DH to form binary physical mixtures at 20% (w/w) intervals from 0 to 100% CBZ DH in the test samples. Each sample was prepared in triplicate and measured by Raman spectroscopy. Ratios of the characteristic spectral intensities based on our previous study (3) were used to construct the calibration models.

Scanning Electron Microscope (SEM)

The solid-state transformation of sample residuals and the surfaces of the drug compacts after solubility and dissolution tests were investigated by SEM. SEM micrographs were photographed by a ZEISS EVO HD 15 scanning electron microscope (Carl Zeiss NTS Ltd., Cambridge, UK). The sample compacts were mounted with Agar Scientific G3347N carbon adhesive tab on Agar Scientific G301 0.5″ aluminium specimen stub (Agar Scientific Ltd., Stansted, UK) and photographed at a voltage of 10.00 kV.

X-ray Powder Diffraction (XRPD)

X-ray powder diffraction patterns of the gel layers of the formulated HPMC matrix tablets after dissolution tests was recorded at a scanning rate of 0.5° 2θ min^{-1} by a Philips automated diffractometer. Cu Kα radiation was used with 40 kV voltage and 35 mA current.

Differential Scanning Calorimetry (DSC)

DSC measurements were conducted for all test samples using a Perkin Elmer Jade DSC (PerkinElmer Ltd., Beaconsfield, UK). The Jade DSC was controlled by Pyris Software. The temperature and heat flow of the instrument were calibrated using an indium and zinc standards. Test samples (8–10 mg) were analysed in crimped aluminium pans with pin-hole pierced lids. Measurements were carried out at a heating rate of 20°C/min under a nitrogen flow rate of 20 ml/min.

Statistical Analysis

The differences in the CBZ solubility and release profiles of CBZ-NIC cocrystal, CBZ III and physical mixture of CBZ III and NIC in aqueous solutions and in HPMC matrices were analysed by on-way analysis variance (ANOVA) (significance level was 0.05) using JMP 11 software. The IDRs of CBZ-NIC cocrystal and CBZ III compacts obtained by UV imaging in each dissolution medium were tested using the same statistical method.

RESULTS

Phase Transformation of CBZ-NIC Cocrystal, CBZ III and Physical Mixture of CBZ III and NIC to CBZ DH in Different Concentrations of HPMC Solutions

Figure 1 shows the CBZ solubility of CBZ-NIC cocrystal, CBZ III and physical mixture of CBZ III and NIC at different HPMC concentration solutions at equilibrium after 24 h. In pure water, there was no significant difference in the equilibrium solubility between CBZ III, CBZ-NIC cocrystal or physical mixture of CBZ III and NIC ($P > 0.05$).

It is revealed that a small amount of HPMC in solution can increase the CBZ solubility of CBZ III and physical mixture of CBZ III and NIC significantly, indicating a higher degree of interaction between CBZ and HPMC to form a soluble complex. No difference in the equilibrium solubility of CBZ III and the physical mixture ($P > 0.05$) at different HPMC concentration solutions was observed, indicating NIC had no effect on the solubility of CBZ because of the low concentration of NIC in the solution, which is consistent with our previous results (5). The solubility of CBZ III or the physical mixture of CBZ III and NIC increased initially with increasing HPMC concentration in solution, to a maximum at 2 mg/ml HPMC concentration and then decreased slightly. This suggests that the soluble complex of CBZ-HPMC reached its solubility limit at 2 mg/ml HPMC in solution. The CBZ solubility of CBZ-NIC cocrystal shows different behaviour to those of CBZ III or the physical mixture ($P < 0.05$), i.e., its value was significantly lower than that of CBZ III and it was
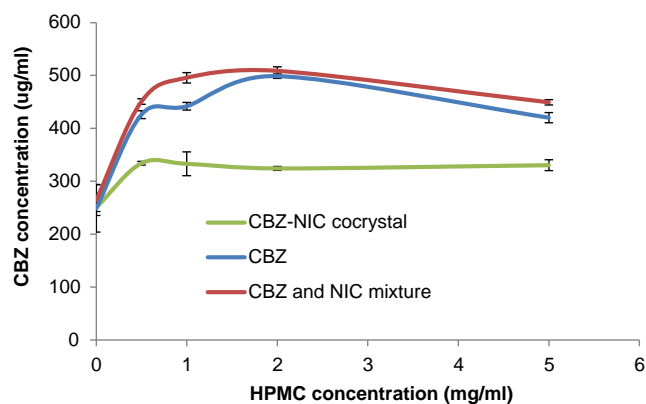

Figure 1 CBZ concentration of CBZ-NIC cocrystal, CBZ III, physical mixture of CBZ III and NIC in different HPMC solution concentration solutions.

nearly constant with increasing HPMC concentrations, indicating the amount of a soluble complex of CBZ-HPMC formed in solution was not significant.

Solid residues retrieved from each of the solubility tests were analysed by DSC, Raman and SEM. The DSC thermographs of the solid residues from different HPMC concentration solutions were examined as shown in Fig. 2(b). The DSC thermographs of individual components are given in Fig. 2(a) for comparison, showing that (i) CBZ III first melted around 165°C and then recrystallized a more stable form CBZ I which melted around 195°C; (ii) the dehydration process of CBZ DH happened during 80–120°C. After dehydration process under DSC heating conditions, CBZ DH converted back to CBZ III which melted around 175°C and recrystallized to CBZ I which melted around 195°C; (iii) NIC melted around 133°C; (iv) CBZ-NIC cocrystal had a single melted point around 163°C; (v) CBZ-NIC physical mixture showed two major thermal events: the first endothermic-exothermic event was around 120–140°C due to melting of NIC and cocrystallisation of CBZ-NIC cocrystal and the second endothermic peak was around 162°C resulting from the melting of newly formed CBZ-NIC cocrystal under DSC heating. Those data are identical to those reported (3,10). It can be clearly seen that the CBZ DH crystals were found in the solid residues of CBZ-NIC cocrystal in different HPMC concentration solutions because there was a clear dehydration process with a sharp endothermic between 80 and 120°C in each DSC thermograph which is analogous to that seen with CBZ DH in Fig. 2(a). This indicates that HPMC did not inhibit the crystallisation of CBZ DH from solution. As expected, the solid residues of CBZ III and the physical mixture in water were converted to CBZ DH after 24 h, showing the same DSC thermographs as that of CBZ DH alone. It can be seen that at 2 mg/ml of HPMC concentration and above, CBZ III alone or in the physical mixture did not convert to dihydrate after 24 h because no dehydration event occurred in the DSC thermographs, indicating that HPMC completely inhibited the transformation of CBZ III to CBZ
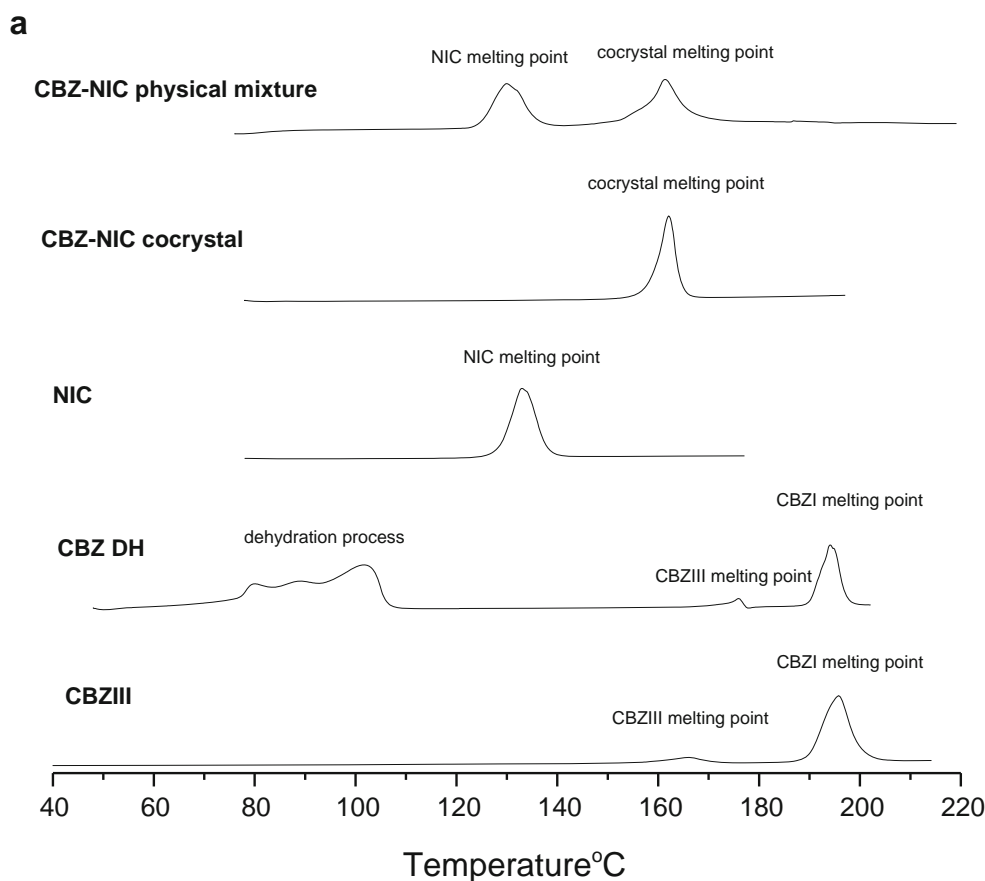
Figure 2 DSC thermographs of solid residues obtained from different HPMC concentration solutions: (**a**) Original samples; (**b**) solid residues.

DH. Furthermore, there were more thermal events occurred at temperature of between 175°C to 185°C, which, we believe, was caused by melting the CBZ IV form and simultaneously recrystallizing to CBZ I.. More discussion will be given in the following section.

Figure 3 shows the influence of different HPMC concentrations on the degree of conversion to CBZ DH analysed by Raman spectroscopy. As expected, the solid residues of CBZ III, CBZ-NIC cocrystal and the physical mixture in water were completely converted to CBZ DH after 24 h. HPMC did not show any influence on the transformation of CBZ-NIC cocrystal to CBZ DH at any concentrations between 0.5 and 5 mg/ml studied, showing the same conversion rate of around 95% CBZ DH in the solid residues. At 2 mg/ml of HPMC concentration and above, conversion rate of CBZ DH for anhydrous CBZ III alone or in physical mixture was zero, which was consistent with the DSC results. The conversion rates of CBZ DH for CBZ III alone and in physical mixture were also same at the other HPMC concentrations, *i.e.*, around 10% in the 0.5 mg/ml HPMC concentration solution and 5% in the 1 mg/ml HPMC concentration solution, indicating HPMC partially inhibited the transformation to CBZ DH. It is also interesting to stress that NIC did not affect the conversion rate for CBZ III in the physical mixture.

Figure 4 shows SEM photographs of solid residues obtained from different HPMC concentration solutions. CBZ III samples used appeared to be prismatic, showing a wide range of size and shape. Small cylindrical NIC particles can be seen to mix with CBZ III particles in the physical mixture samples. CBZ-NIC cocrystals show thin needle-like shape with a wide range of size distribution. It can be seen that HPMC has a significant influence on the morphology of the crystals shown in SEM photographs. In water, prism-like CBZ III crystals have transferred into needle-like CBZ DH crystals. At different HPMC concentration solutions, there was no significant change of the morphology for most of the residual crystals compared with the starting materials of CBZ III, however, it can clearly be seen that some spherical aggregates appeared to be amorphous in the residuals, all of which are consistent with previous findings (9). The similar morphology of the residues as those of CBZ III in different concentration of HPMC solutions can be found for physical mixture of CBZ III and NIC, indicating that all of NIC samples have dissolved and there is no effect of NIC on the phase transformation of CBZ III. For the CBZ-NIC cocrystals, the residues in up to 1 mg/ml HPMC concentration solutions show the needle-like shape as that of pure CBZ DH whose size distribution is much more even and narrow than that of the CBZ-NIC
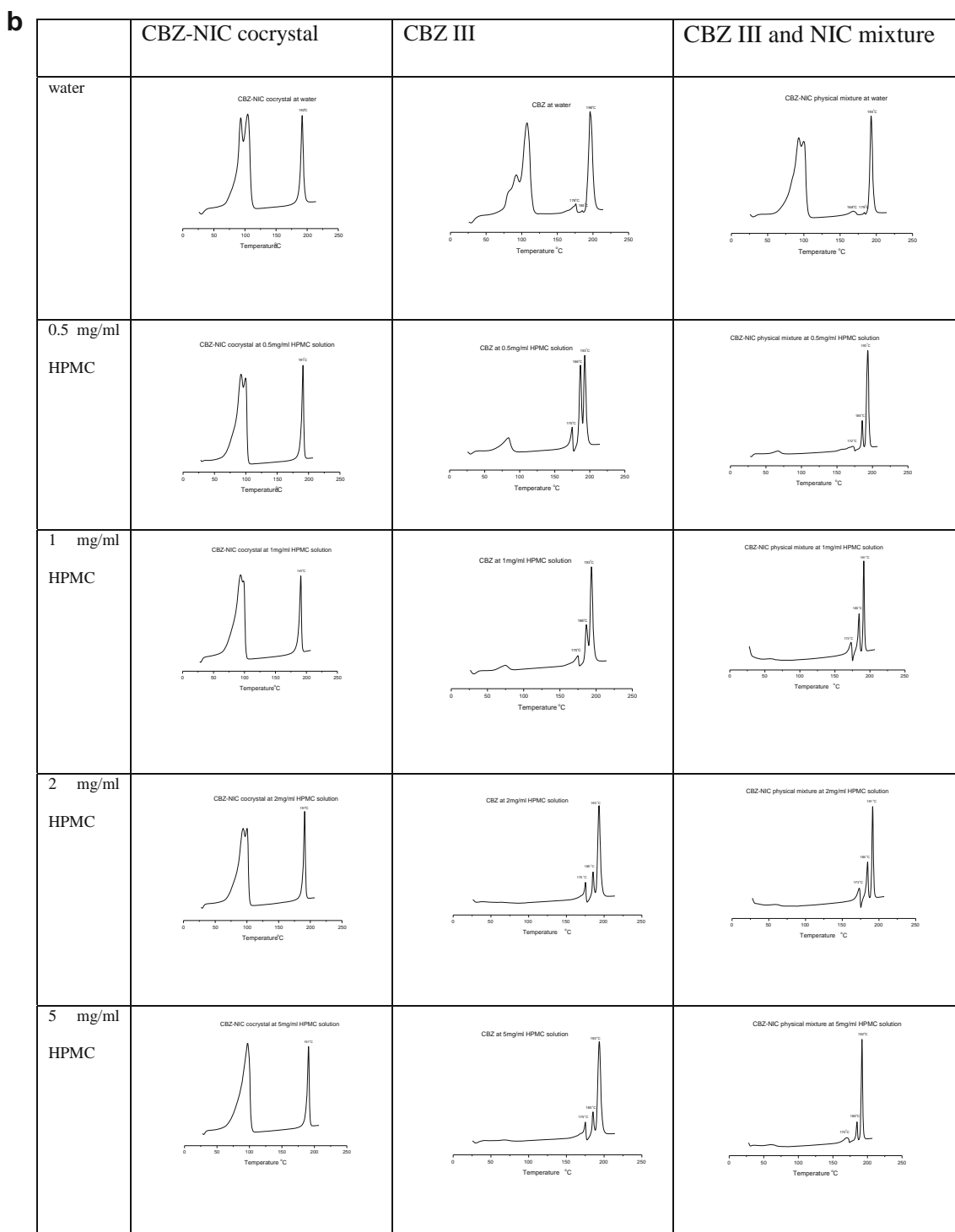
Fig. 2 (continued)

cocrystals, indicating HPMC did not inhibit the crystallisation of CBZ DH from the solution. At concentrations of 2 and 5 mg/ml HPMC solutions, the crystals of CBZ DH were thicker than the CBZ DH crystals precipitated from pure water and some aggregates composed of small crystals also appeared with needle-like shape of CBZ DH crystals.

The IDR profiles from the compacts of the CBZ III (dashed lines) and CBZ-NIC cocrystal (solid lines) at different HPMC concentration dissolution media are shown in Fig. 5. A video clip of CBZ-NIC cocrystal dissolution at the 2 mg/ml HPMC dissolution medium can be found in the Supplementary Material. It can be seen that all IDRs

decreased quickly within 10 min and reached its static values after 30 min. It has been found that there is no difference of the IDR profiles of the CBZ-NIC cocrystal at different HPMC concentration dissolution media ($P>0.05$). Prior to the dissolution tests, all of the compact surfaces of CBZ-NIC cocrystals were smooth. After the dissolution tests, the SEM photographs (Fig. S1 in the Supplementary Material) show that small needle-shaped CBZ DH crystals have appeared on the compact surfaces of the CBZ-NIC cocrystals, indicating HPMC did not inhibit the recrystallization of CBZ DH crystals from the solutions. Different dissolution behaviour ($P<0.05$) of CBZ III at different HPMC concentration dissolution media was found. When the dissolution medium was water, the IDR of CBZ III decreased quickly due to precipitation of CBZ DH on the compact surface (shown in the SEM photographs in Fig. S1 in the Supplementary Material). The IDR of CBZ III increased significantly when the HPMC was added in the dissolution medium in Fig. 5 and there were no CBZ DH crystals on the compact surfaces in Fig. S1 in the Supplementary Material, indicating HPMC inhibited the recrystallization of CBZ DH crystals from the solutions. It can be also shown that the CBZ-NIC cocrystal has an improved dissolution rate in water when compared with CBZ III, however, its advantage has been completely lost (when compared with CBZ III) when HPMC is included in a dissolution medium.
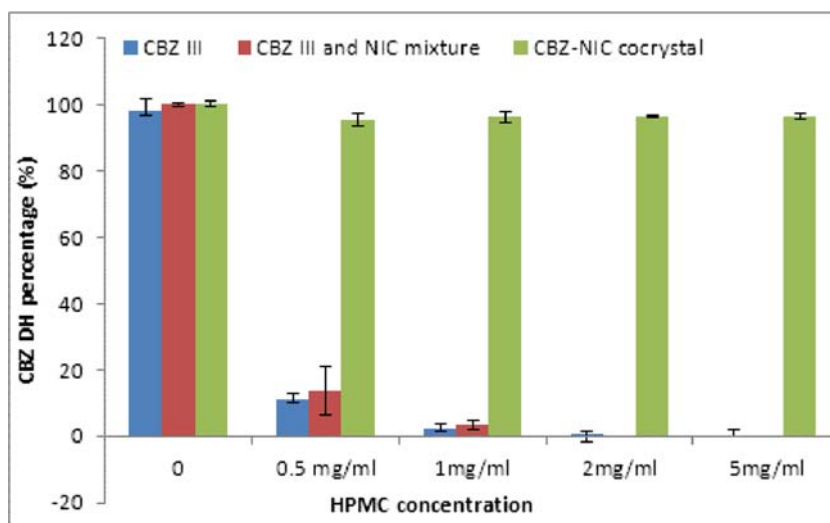
CBZ Release Profiles of CBZ-NIC Cocrystal, CBZ III and Physical Mixture of CBZ III and NIC in HPMC Matrices

Figure 6(a) presents the CBZ release profiles of the CBZ-NIC cocrystal, CBZ III and a physical mixture of CBZ III and NIC from the 100 mg HPMC matrices. It is shown that the CBZ release from the CBZ-NIC cocrystal formulation is significant different from those of the CBZ III and physical mixture

formations ($P<0.05$). It is interesting to note that the significantly higher release of CBZ from the CBZ-NIC cocrystal formulation was found at the early stage of the dissolution (up to 1 h). However, the CBZ release rate from the cocrystal formulation changed significantly and gradually decreased to be a lower value than those of the CBZ III and physical mixture formulations after 2.5 h, indicating significantly changes to the cocrystal properties in the matrix. The difference on the CBZ releases from the CBZ III and physical mixture formulations was found to be significant during dissolution up to 3 h ($P<0.05$) and after that the CBZ release profiles from the both formulations were same ($P>0.05$). It can be seen that up to 1 h of the dissolution test the CBZ release rate from the CBZ III formulation was lowest, which can properly be explained by the initially slower hydration and gel layer formation processes of HPMC. Once hydration process of the tablet has completed the CBZ release rate kept constant. For the physical mixture of CBZ and NIC formulation, the hydration and gel layer formation processes of HPMC was much faster than the CBZ III alone formulation because of the quickly dissolved NIC as a channel agent to speed up the water uptake process, resulting in a higher release rate. Once all of NIC dissolved, both of formations showed a similar dissolution profile.

Figure 6(b) presents the CBZ release profiles of CBZ-NIC cocrystal, CBZ III and physical mixture of CBZ III and NIC from the 200 mg HPMC matrices. Overall, the results show that increasing HPMC in a formulation resulted in the reduced CBZ release rate for all three formulations, indicating HPMC slowed down the drug dissolution. It is revealed that the CBZ release from the CBZ-NIC cocrystal formulation is much higher than the other two formulations of CBZ III and physical mixture, showing the advantage of CBZ-NIC cocrystal formulation. Incorporation of NIC in the formulation gave no change of the CBZ III release rate ($P>0.05$),

Figure 3 Influence of HPMC concentration on conversion of CBZ to CBZ DH after 24 h.

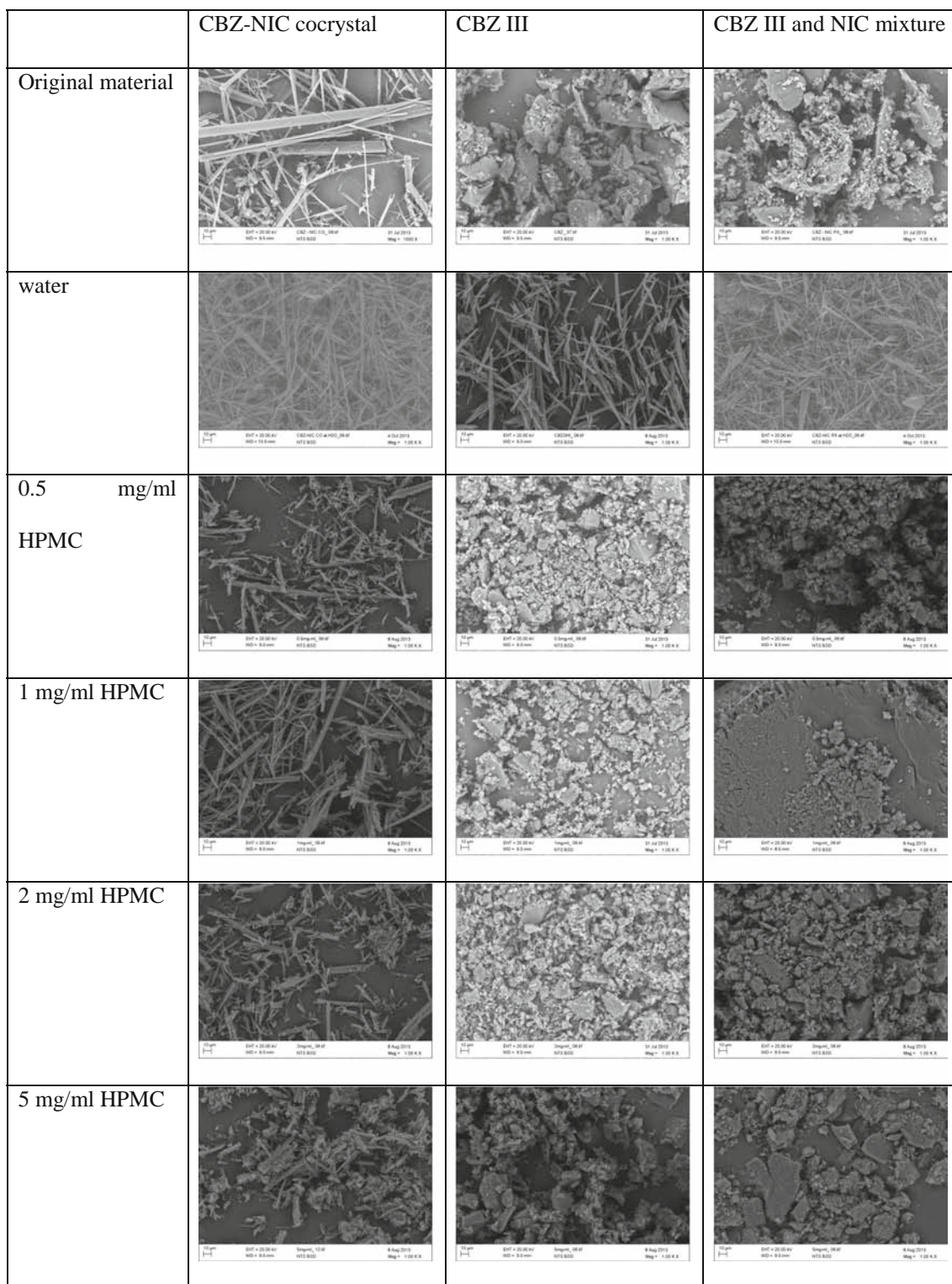|	CBZ-NIC cocrystal	CBZ III	CBZ III and NIC mixture
Original material			
water			
0.5 mg/ml HPMC			
1 mg/ml HPMC			
2 mg/ml HPMC			
5 mg/ml HPMC			

Figure 4 SEM photographs of solid residues obtained from different HPMC concentration solutions.

demonstrating no effect of NIC on the enhancement of CBZ III dissolution in the formation. The CBZ release from each of three formulations was nearly constant.

In order to understand the mechanisms involved in the CBZ release of CBZ-NIC cocrystal from a HPMC matrix, the solid crystal properties in the gel layer were examined using XRPD, SEM and DSC.

Figure 7(e)–(j) present the corresponding XRPD patterns of the crystals in the gel layers of different formulations. The XRPD patterns of individual components of CBZ III, CBZ
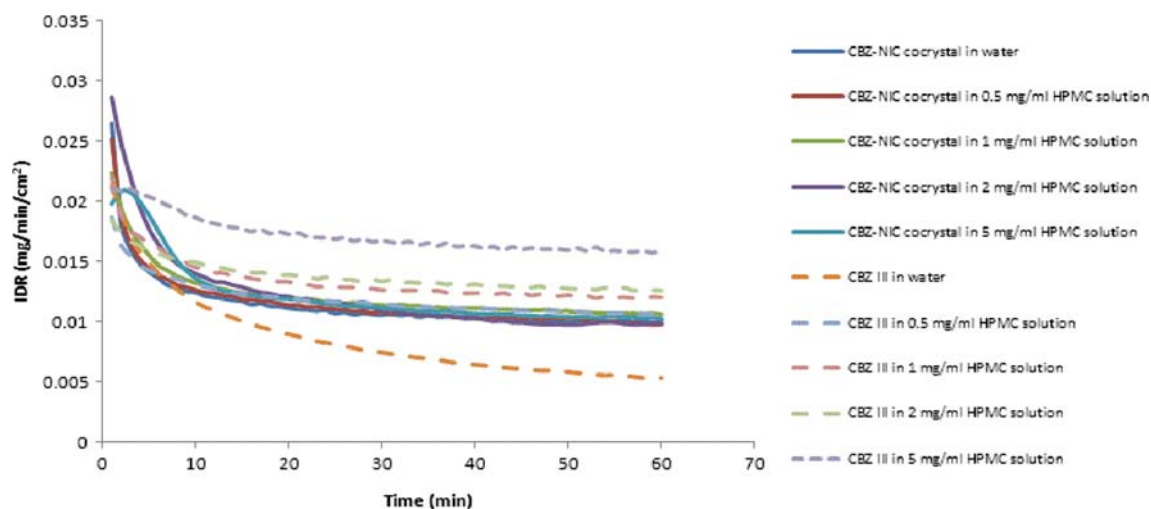
Figure 5 Intrinsic dissolution rates obtained by UV imaging ($n = 3$).

DH, NIC and CBZ-NIC cocrystal are also presented in Figure 7(a)–(d). The characteristic diffraction peaks of CBZ III are at $2\theta = 13.1°$, $15.3°$, $19.6°$, and $20.1°$, identical to those of reported data (10–13). The reflections at $9.0°$, $12.4°$, $18.8°$ and $19.0°$ are especially characteristic peaks of CBZ DH. NIC shows the characteristic diffraction peaks at $2\theta = 14.9°$ and $23.5°$. The characteristic diffraction peaks of CBZ-NIC cocrystal are exhibited at $2\theta = 6.7°$, $9.0°$, $10.3°$, $13.5°$, and $20.6°$ in agreement with previous reports (11,14).

Figure 6 CBZ release profiles of CBZ-NIC cocrystal, CBZ III and physical mixture of CBZ III and NIC formulations: (**a**) in 100 mg HPMC matrix; (**b**) in 200 mg HPMC matrix.
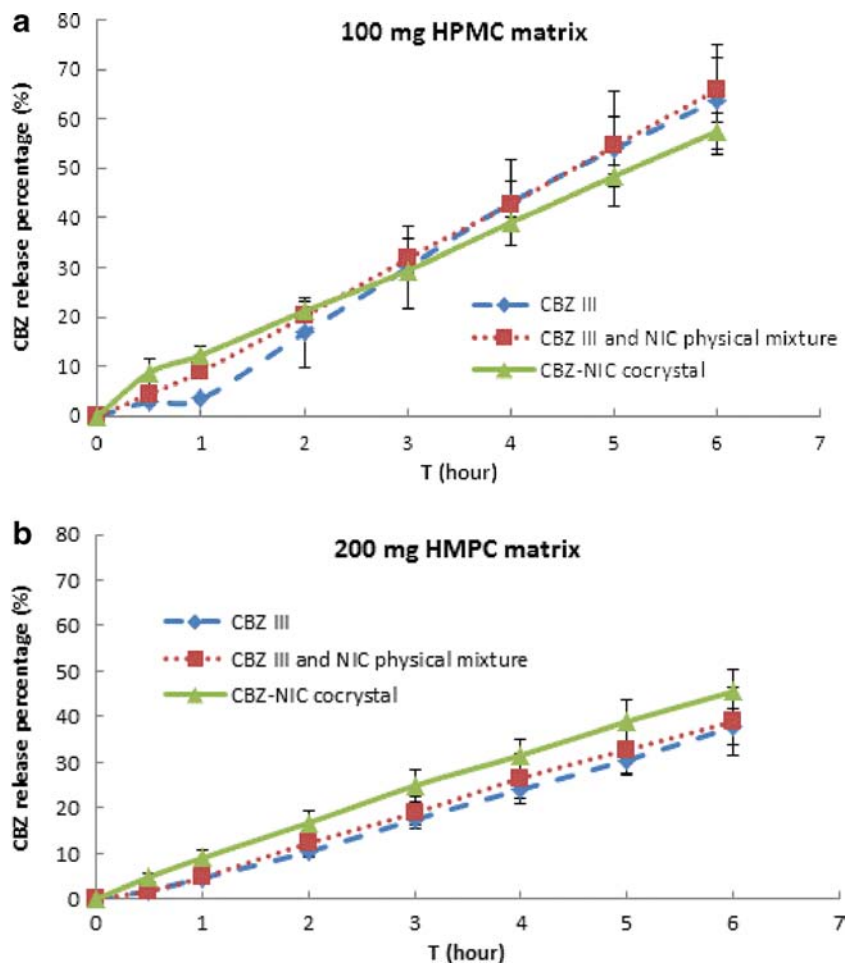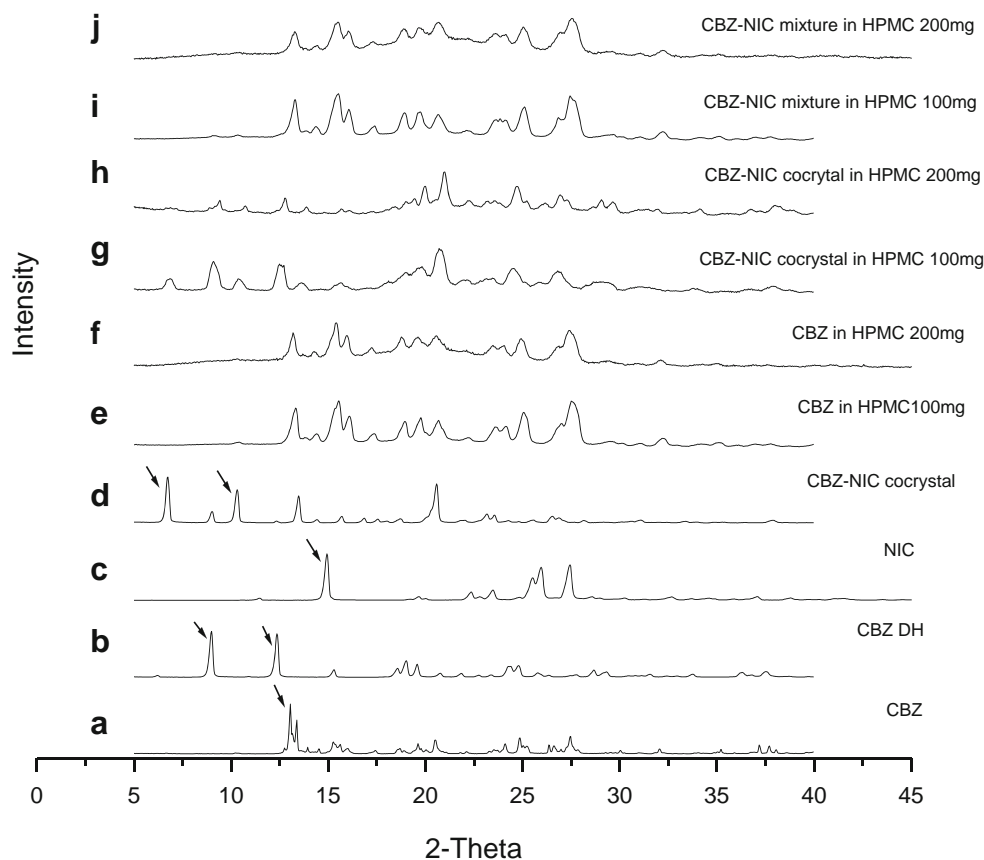
Figure 7 XRPD patterns.

The significant and strong characteristic peaks of CBZ III, without any characteristic peaks of CBZ DH, were observed in the gels of CBZ III tablets in both 100 mg and 200 mg HPMC matrices, implying that there was no change of CBZ III crystalline state. In the gel layers of physical mixture of CBZ III and NIC in both 100 mg and 200 mg matrices, it only shows the characteristic peaks of CBZ III and no diffraction peaks of NIC or CBZ DH are found, indicating NIC has dissolved completely and there is no effect of its existence in the formulation on the crystalline properties of CBZ III. Furthermore, the XRPD diffraction patterns of CBZ III obtained from the formulations of CBZ III and physical mixture of CBZ III and NIC in Fig. 7(e), (f), (i) and (j) revealed the characteristic peaks of CBZ IV at $2\theta = 14.4$ and $17.4°$ (10), indicating a new form of CBZ IV crystallised during the dissolution of tablets. In the meantime, the XRPD diffraction patterns showed significantly the weaker and broader peaks compared with that of CBZ III powder in Fig. 7(a), which could be attributed to its smaller particle in size and a complex interaction between CBZ III and HPMC on the molecular scale during the dissolution process. With both CBZ-NIC cocrystal and CBZ DH characteristic peaks are observed in the CBZ-NIC cocrystal formulations of 100 mg and 200 mg HPMC matrices, indicating recrystallization of CBZ DH from the solution. However, diffraction peaks of CBZ DH in

100 mg HPMC matrix are stronger, indicating more CBZ DH has been recrystallized. The broad peaks of CBZ DH obtained compared with the X-ray patterns of pure CBZ DH indicated a decrease in crystallinity of the crystals with the formation of less ordered structure.

The SEM morphologies of the gels after the dissolution tests are shown in Fig. 8. It is clearly shown that there are many CBZ DH particles dispersed in the gels for the CBZ-NIC cocrystal formulations in both 100 mg and 200 mg HPMC matrices and needle-shaped CBZ DH particles were not found in a formulation of either CBZ III or physical mixture of CBZ III and NIC.

DSC results also show the similar results in Fig. S2 in the Supplementary Material, supporting XRPD and SEM analysis.

DISCUSSION

The inhibition of CBZ III phase transition to CBZ DH and the amorphism induced in the presence of low concentrations of HPMC and in the gel layer of hydrated tablets has been studied extensively (9). It is known that the hydroxyl groups of HPMC attach to CBZ at the site of water binding and therefore its transformation to the dihydrate form is inhibited.
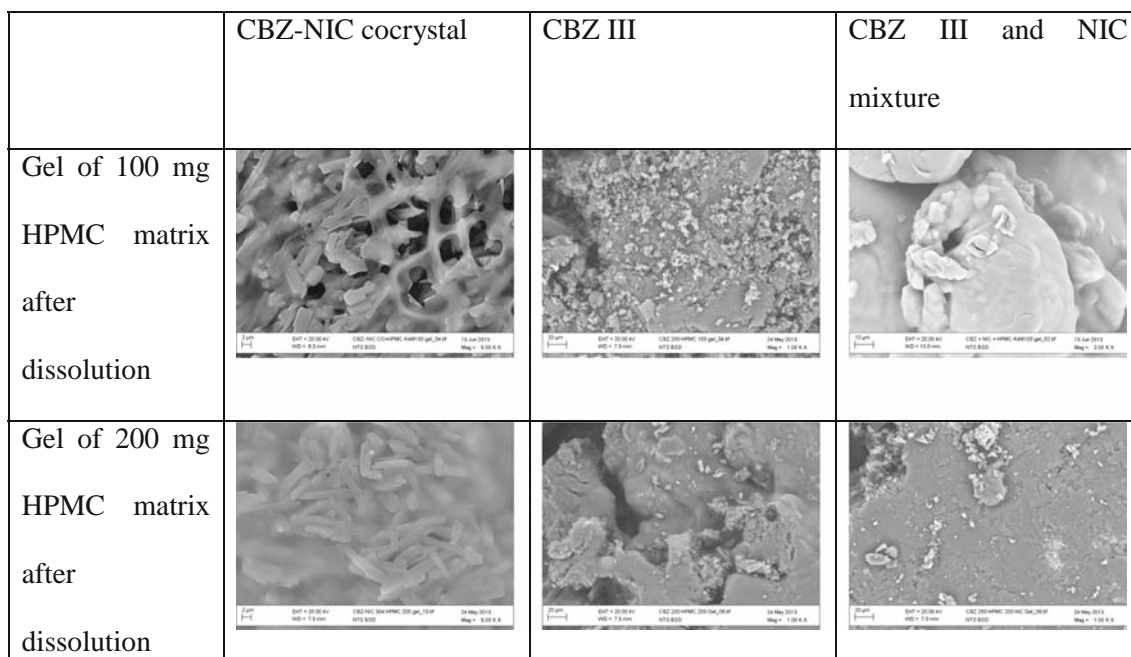
	CBZ-NIC cocrystal	CBZ III	CBZ III and NIC mixture
Gel of 100 mg HPMC matrix after dissolution			
Gel of 200 mg HPMC matrix after dissolution			

Figure 8 SEM photographs of gel layers after dissolution tests.

In this study it was initially expected that HPMC would also inhibit the transformation of CBZ-NIC cocrystal to CBZ DH during dissolution because the change of crystalline properties of CBZ-NIC cocrystal during dissolution can reduce the advantages of the improved dissolution rate and solubility, resulting in a poor drug absorption and bioavailability (3,5). Unfortunately, the study has shown that HPMC did not inhibit the phase transformation of CBZ-NIC cocrystal to CBZ DH in both the aqueous solutions and sustained release HPMC matrix tablets. It also indicated that the CBZ release profile of CBZ-NIC cocrystal was significantly affected by the percentage of HPMC in the formulation.

In fusion, the competition mechanism between CBZ and NIC with HPMC to form hydrogen bonds has been proposed (11). When the physical mixture of CBZ III, NIC and HPMC was heated up, NIC was molten first and then both CBZ III and HPMC can dissolve in molten NIC and form intermolecular hydrogen bonds between three components (15).

In solution, the situation is different and is complicated with not only solute-solute and solute-solvent interactions but also rates of dissolution of solids into the solution and rates of association of components in the solution.

In the solubility study of CBZ III in different concentrations of HPMC solutions, it was found that the apparent solubility CBZ initially increased with increasing concentration of HPMC in solution shown in Fig. 1, indicating a soluble complex formation between CBZ and HPMC in solution. When the concentration of HPMC was higher than 1 mg/ml, the solubility limit of the complex formed was reached and the total apparent solubility of CBZ in solution did not change significantly, as shown by the plateau in Fig. 1.

The sole phase of CBZ III was shown in the solid residues when the concentration of HPMC was above 1 mg/ml shown in Figs. 2 and 3 by DSC and Raman spectroscopy, indicating that HPMC can inhibit the precipitation of CBZ DH. A reasonable explanation is probably twofold and due to: 1) stronger interaction between CBZ and HPMC involving hydrogen bonding interaction occurring at the site where water molecules attack CBZ to form a CBZ-HPMC association, resulting in inhibition of the formation of CBZ DH in solution and 2) the formation of the soluble complex of CBZ-HPMC in the solution was faster than the rate of CBZ III dissolution. When the HPMC concentration was higher than 2 mg/ml, the solubility limit of the complex of CBZ-HPMC formed was exceeded, resulting in the precipitation of the complex of CBZ-HPMC showing induction of amorphism of CBZ III crystals in the solid residues. Therefore, the apparent CBZ solubility decreased, shown in Fig. 1. SEM images in Fig. 4 show larger agglomerated particles in the solid residuals of 5 mg/ml HPMC solution. The UV imaging intrinsic dissolution study of CBZ III compacts has also supported the above explanation. When the dissolution medium was water, the IDR of CBZ III decreased quickly due to precipitation of CBZ DH on the compact surface because of supersaturation of the CBZ solution around the compact surface. The IDRs of CBZ III increased with increasing HPMC concentration and there was no CBZ DH precipitated on the sample compact surface when HPMC was included in the dissolution media. The same CBZ solubility profile of the physical mixture of CBZ III and NIC was obtained, suggesting that NIC has not been incorporated into the complex with CBZ or HPMC in solution. The reason is that the interaction force between NIC

and water is much stronger than the other two components, as a result of the large incongruent solubility difference between NIC and CBZ or HPMC in water. This is consistent with our previous report (5), in which at a low NIC concentration (up to 40 mM) there was on soluble complex of NIC and CBZ formed in solution.

The apparent CBZ solubility of CBZ-NIC cocrystal was same as the solubility of CBZ III alone or physical mixture of CBZ III and NIC because the interaction force of CBZ and NIC was much weaker that of NIC with water, resulting in failing in formation of the soluble complex of CBZ-NIC at a low concentration of NIC. The apparent CBZ solubility of CBZ-NIC cocyrstal at different concentration of HPMC solutions was constant and increased slightly compared with that of CBZ-NIC cocrystal in water. This can be explained by the rate differences between the cocrystal dissolution and formation of a soluble complex of CBZ and HPMC in solution. The CBZ-NIC cocrystal has a higher solubility and faster dissolution rate, therefore, higher supersaturation of CBZ in solution can be generated during dissolution. Although the soluble complex of CBZ-HPMC can be formed to stabilize CBZ in the solution, the rate of CBZ from the dissolved CBZ-NIC cocrystal entering into the solution was much faster than the rate of the CBZ-HPMC complex formation, leading to precipitation of CBZ DH. Raman analysis shown in Fig. 3 has indicated that nearly 95% of CBZ DH crystals in the solid residues and SEM images in Fig. 4 show the needle-shaped particles precipitated on the surfaces of sample compacts. The IDR profiles of CBZ-NIC cocrystal compacts at different concentrations of HPMC dissolution media were same shown in Fig. 5, indicating failure of formation of CBZ-HPMC complex to stabilize the CBZ in the dissolution media, resulting in the precipitation of CBZ DH crystals on the surfaces of the compacts shown in Fig. S1 in the Supplementary Material.

Study has shown that CBZ IV (C-monoclinic) can be crystallized by slow evaporation of an ethanol solution in the presence of polymers, such as hydroxypropyl cellulose, poly(4-methylpentene), poly(α-methylstyrene), and poly(p-phenylene ether-sulfone) (10,16). In this study, it indicated that CBZ IV can also be crystallized by dissolving CBZ III in HPMC solutions. The DSC results of the solid residues from the both CBZ III and physical mixture of CBZ III and NIC in different concentrations of HPMC solutions in Fig. 2(b) have revealed an additional endothermic-exothermic thermal event between 175 and 185°C corresponding to the melting point of CBZ IV (10), indicating HPMC has been docked on the surfaces of CBZ III crystalsas heteronucleito induce defects of crystallinity. Although some aggregates appeared in the solid residuals of CBZ-NIC cocrystal at different concentration of HPMC solutions, the DSC thermograms are same shown in Fig. 2, indicating HPMC was not crystallised in the crystal units of CBZ dihydrate, however, it affected the morphology of CBZ DH crystals.

When the CBZ-NIC cocrystal was formulated into sustained release HPMC matrix tablets, the change of the crystalline properties of the cocrystal was affected not only by interaction forces among the components in solution but also by the matrix hydration and erosion characteristics of the drug delivery system. It is revealed that depression of CBZ-NIC cocrystal dissolution by HPMC was affected by drug loading. The higher drug loading resulted in weaker depression effect, showing high CBZ release rates for all three formulations at 100 mg HPMC matrices.

In a lower percentage of 100 mg HPMC matrixes, the CBZ release profiles of CBZ-NIC cocrystal, CBZ III and physical mixture show the similar behaviour as their IDRs in solution in our previous study (3). The CBZ-NIC cocrystal in 100 mg HPMC matrix has shown the highest release rate compared with the other two formulations at the early stage of the dissolution up to 2 h because of improved dissolution rate and solubility of CBZ-NIC cocrystal. The study has shown that the solubility of CBZ-NIC was ca. 130 to 319 times that of CBZ III alone in water (5). However, the dissolution profile of CBZ-NIC cocrystal was nonlinear and the release rate declined over time. The XRPD analysis of the gel layer has shown that CBZ DH crystals have recrystallized from the solution. Similar as the solubility study of the CBZ-NIC cocrystal, HPMC in solution failed to stabilize CBZ in solution because of a slower formation rate of the soluble complex of CBZ-HPMC compared with a faster dissolution rate of CBZ-NIC cocrytal. Because of solid phase transformation of CBZ-NIC cocrystal, the CBZ release rate from the cocrystal formation was lower than that of the formation of CBZ III alone or physical mixture after 2 h in the dissolution tests.

In contrast, the CBZ release rate from the physical mixture in the HPMC matrix was linear. When the more soluble component of NIC dissolved rapidly from the matrix, pores can be formed to bring more water into the matrix to increase the dissolution rate of both HPMC and CBZ, showing higher CBZ dissolution rate compared with that of pure CBZ III formulation. A significant delay release stage from the pure CBZ III formulation was observed because of the hydration of the HPMC matrix. When NIC dissolved and the HPMC matrix was hydrated, the two formulations showed the same CBZ release rates.

With an increased HPMC content in the tablets, it was observed that the release rate of CBZ from different formulations was reduced. The CBZ release profiles of CBZ-NIC cocrystal, CBZ III and physical mixture in the 200 mg HPMC matrix tablets were controlled mainly by the matrix bulk erosion, indicating zero order kinetics of CBZ release rate. Although the XRPD diffraction patterns of the gels of the CBZ-NIC cocrystal formulation show the crystallisation of CBZ DH crystals, the CBZ release is less influenced by the change of the crystalline properties of CBZ-NIC cocrystal. When a matrix tablet is immersed in the dissolution medium,

wetting occurs at the surface and then progresses into the matrix to form an entangled three-dimensional gel structure in HPMC. Molecules undergoing chain entanglement are characterized by strong viscosity dependence on concentration. An increase in the HPMC percentage in the formulation can lead to an increase in the gel viscosity, suppressing the dissolution of the CBZ-NIC cocrystal. Dissolution of most of CBZ-NIC cocrystals can only occur at the outer surface of the matrix when HPMC undergoes a process of disentanglement in order to be released from the matrix. A similar hydration process also occurred for the CBZ III and physical formulations in 200 mg HPMC matrices. Therefore the CBZ release from the CBZ-NIC cocrystal formulation is much higher than the other two formulations.

After 6 h dissolution tests, the matrices of the six formulations maintained their structural integrity. XRPD diffraction patterns of CBZ III obtained from the formulations of CBZ III and physical mixture of CBZ III and NIC revealed the defect of crystallinity because CBZ IV appeared in the gel layers, indicating the weaker and broader peaks compared with CBZ III powder. The broad peaks of CBZ DH obtained from the gel of CBZ-NIC cocrystal formulations compared with those of pure CBZ DH indicated a change in the crystallinity of crystals with the formation of less ordered structure.

CONCLUSIONS

The influence of HPMC on the phase transformation and release profiles of CBZ-NIC cocrystal in solution and in sustained release matrix tablets has been investigated using DSC, XRPD, Raman spectroscopy and UV imaging. The results have indicated that HPMC cannot inhibit the transformation of CBZ-NIC cocrystal to CBZ DH in solution or in the gel layer of the matrix, in contrast with its ability of the inhibition of CBZ III phase transition to CBZ DH. The mechanism of HPMC incapability for inhibition of CBZ dihydrate during CBZ-NIC cocrystal dissolution is caused by the rate differences between CBZ-NIC cocrystal dissolution and formation of a CBZ-HPMC soluble complex in the solution. For CBZ III alone or a physical mixture of CBZ III and NIC, the rate of CBZ III dissolution was slower than the rate of formation of a CBZ-HPMC association in solution, involving a hydrogen bonding interaction at the site where water molecules attach CBZ. The supersaturation level of the soluble complex of CBZ-HPMC was exceeded first, causing the precipitation of CBZ IV crystals with HPMC docked on the surfaces of CBZ III crystals and hence to induce imperfection during the crystal formation. Because of the significantly improved dissolution rate of CBZ-NIC cocrystal, the rate of CBZ entering into the solution was significantly faster than the rate of the formation of the CBZ-HPMC soluble complex, leading to high supersaturation levels of CBZ and

subsequently precipitation of CBZ DH. Therefore, the apparent solubility and dissolution rate of CBZ of CBZ-NIC cocrystal were constant at different concentration of HPMC solutions. In a lower percentage of 100 mg HPMC matrixes, the CBZ release profile of CBZ-NIC cocrystal was nonlinear and declined over time, which was affected significantly by the change of the crystalline properties of CBZ-NIC cocrystal. With an increased HPMC content in the tablets, dissolution of CBZ-NIC cocrystal can only occur at the outer surface of the matrix when HPMC undergoes a process of disentanglement, showing significantly higher CBZ release rate in comparison with the other two formulations of CBZ III and physical mixture. In conclusion, it is undoubted that cocrystals can offer great advantage to fine-tune physicochemical properties of drug compounds, in particular, improved solubility and dissolution rate of poorly water soluble drugs. However, how to maintain drug supersaturation level after dissolution of cocrystalsis is a huge task and needs more research. In the meantime, it is anticipated that the pharmaceutical cocrystals can cause more variety in *in vivo* dissociation due to its complexity. More work should be carried out to investigate the correlation between *in vitro* and *in vivo* dissolution of cocrystals.

REFERENCES

1. Thakuria R, Delori A, Jones W, Lipert MP, Roy L, Rodríguez-Hornedo N. Pharmaceutical cocrystals and poorly soluble drugs. Int J Pharm. 2013;453:101–25.
2. Qiao N, Li M, Schlindwein W, Malek N, Davies A, Trappitt G. Pharmaceutical cocrystals: an overview. Int J Pharm. 2011;419:1–11.
3. Qiao N, Wang K, Schlindwein W, Davies A, Li M. In situ monitoring of carbamazepine-nicotinamide cocrystal intrinsic dissolution behaviour. Eur J Pharm Biopharm. 2013;83:415–26.
4. Remenar JF, Peterson ML, Stephens PW, Zhang Z, Zimenkov Y, Hickey MB. Celecoxib: nicotinamide dissociation: using excipients to capture the Cocrystal's potential. Mol Pharm. 2007;4:386–400.
5. Li M, Qiao N, Wang K. Influence of sodium lauryl sulphate and tween 80 on carbamazepine-nicotinamide cocrystal solubility and dissolution behaviour. Pharmaceutics. 2013;5:508–24.
6. Huang N, Rodríguez-Hornedo N. Engineering cocrystal solubility, stability, and pH max by micellar solubilization. J Pharm Sci. 2011;100:5219–34.
7. Kovačević I, Parojčić J, Homšek I, Tubić-Grozdanis M, Langguth P. Justification of biowaiver for carbamazepine, a Low soluble high permeable compound, in solid dosage forms based on IVIVC and gastrointestinal simulation. Mol Pharm. 2008;6:40–7.
8. Childs SL, Wood PA, Rodriguez-Hornedo NR, Reddy LS, Hardcastle KI. Analysis of 50 crystal structures containing carbamazepine using the materials module of mercury CSD. Cryst Growth Des. 2009;9:1869–88.
9. Katzhendler I, Azoury R, Friedman M. Crystalline properties of carbamazepine in sustained release hydrophilic matrix tablets based on hydroxypropyl methylcellulose. J Control Release. 1998;54:69–85.
10. Grzesiak AL, Lang M, Kim K, Matzger AJ. Comparison of the four anhydrous polymorphs of carbamazepine and the crystal structure of form I. J Pharm Sci. 2003;92:2260–71.

11. Liu X, Lu M, Guo Z, Huang L, Feng X, Wu C. Improving the chemical stability of amorphous solid dispersion with cocrystal technique by hot melt extrusion. Pharm Res. 2012;29:806–17.
12. Lehto P, Aaltonen J, Tenho M, Rantanen J, Hirvonen J, Tanninen VP, et al. Solvent-mediated solid phase transformations of carbamazepine: effects of simulated intestinal fluid and fasted state simulated intestinal fluid. J Pharm Sci. 2009;98: 985–96.
13. Gagnière E, Mangin D, Puel F, Rivoire A, Monnier O, Garcia E, et al. Formation of co-crystals: kinetic and thermodynamic aspects. J Cryst Growth. 2009;311:2689–95.
14. Seefeldt K, Miller J, Alvarez-Núñez F, Rodríguez-Hornedo N. Crystallization pathways and kinetics of carbamazepine–nicotinamide cocrystals from the amorphous state by in situ thermomicroscopy, spectroscopy, and calorimetry studies. J Pharm Sci. 2007;96:1147–58.
15. Hinoand T, Ford JL. Characterization of the hydroxypropyl methylcellulose-nicotinamide binary system. Int J Pharm. 2001;219: 39–49.
16. Lang M, Grzesiak AL, Matzger AJ. The Use of polymer heteronuclei for crystalline polymorph selection. J Am Chem Soc. 2002;124: 14834–5.